

Canonical seesaw implication for two-component dark matter

Phung Van Dong,* Cao H. Nam,† and Duong Van Loi‡
*Phenikaa Institute for Advanced Study and Faculty of Basic Science,
 Phenikaa University, Yen Nghia, Ha Dong, Hanoi 100000, Vietnam*
 (Dated: April 1, 2021)

We show that the canonical seesaw mechanism implemented by the $U(1)_{B-L}$ gauge symmetry provides two-component dark matter naturally. The seesaw scale that breaks $B-L$ defines a residual gauge symmetry to be $Z_6 = Z_2 \otimes Z_3$, where Z_2 leads to the usual matter parity, while Z_3 is newly recognized, transforming quark fields nontrivially. The dark matter components—that transform nontrivially under the matter parity and Z_3 , respectively—can gain arbitrary masses, despite the fact that the Z_3 dark matter may be heavier than the light quarks u, d . This dark matter setup can address the XENON1T anomaly recently observed and other observables, given that the dark matter masses are nearly degenerate, heavier than the electron and the $B-L$ gauge boson Z' , as well as the fast-moving Z_3 dark matter has a large $B-L$ charge, while the Z' is viably below the beam dump experiment sensitive regime.

PACS numbers: 12.60.-i

Motivation. Neutrino mass and dark matter are the two big questions in science, which require the new physics beyond the standard model [1].

It is well established that the canonical seesaw mechanism can generate appropriate small neutrino masses through the exchange of heavy Majorana right-handed neutrino singlets, ν_{aR} for $a = 1, 2, 3$, added to the standard model [2–10]. However, the canonical seesaw in its simple form does not naturally address the dark matter issue, unless some dark matter stability condition or parameter finetuning is *ad hoc* imposed.

The simplest gauge completion of the seesaw mechanism with $U(1)_{B-L}$ can provide a natural origin for the existence of the right-handed neutrinos and the right-handed neutrino mass scale [11–13]. This work shows that such theory manifestly yields a novel consequence of two-component dark matter, properly solving the recent XENON1T excess [14].

Description of the model. Indeed, the full gauge symmetry takes the form,

$$SU(3)_C \otimes SU(2)_L \otimes U(1)_Y \otimes U(1)_{B-L}. \quad (1)$$

Here the right-handed neutrino fields ν_{aR} transforming under the gauge symmetry as

$$\nu_{aR} \sim (1, 1, 0, -1) \quad (2)$$

are required in order to cancel the $[\text{Gravity}]^2 U(1)_{B-L}$ and $[U(1)_{B-L}]^3$ anomalies. Additionally, a scalar singlet transforming under the gauge symmetry as

$$\chi \sim (1, 1, 0, 2) \quad (3)$$

must be presented to break $U(1)_{B-L}$ for the model consistency, simultaneously generating the right-handed neutrino masses or the seesaw scale.

As usual, let us assign the standard model lepton, quark, and Higgs representations with respect to the new gauge symmetry to be,

$$l_{aL} = \begin{pmatrix} \nu_{aL} \\ e_{aL} \end{pmatrix} \sim \left(1, 2, -\frac{1}{2}, -1\right), \quad (4)$$

$$e_{aR} \sim (1, 1, -1, -1), \quad (5)$$

$$q_{aL} = \begin{pmatrix} u_{aL} \\ d_{aL} \end{pmatrix} \sim \left(3, 2, \frac{1}{6}, \frac{1}{3}\right), \quad (6)$$

$$u_{aR} \sim \left(3, 1, \frac{2}{3}, \frac{1}{3}\right), \quad (7)$$

$$d_{aR} \sim \left(3, 1, -\frac{1}{3}, \frac{1}{3}\right), \quad (8)$$

$$\phi = \begin{pmatrix} \phi^+ \\ \phi^0 \end{pmatrix} \sim \left(1, 2, \frac{1}{2}, 0\right). \quad (9)$$

The scalar multiplets develop vacuum expectation values (VEVs), such as

$$\langle \chi \rangle = \frac{\Lambda}{\sqrt{2}}, \quad \langle \phi \rangle = \begin{pmatrix} 0 \\ \frac{v}{\sqrt{2}} \end{pmatrix}, \quad (10)$$

satisfying

$$\Lambda \gg v = 246 \text{ GeV}. \quad (11)$$

The Yukawa Lagrangian includes

$$\begin{aligned} \mathcal{L} \supset & h_{ab}^\nu \bar{l}_{aL} \tilde{\phi} \nu_{bR} + \frac{1}{2} f_{ab}^\nu \bar{\nu}_{aR}^c \chi \nu_{bR} + H.c. \\ & \supset -\frac{1}{2} (\bar{\nu}_{aL} \bar{\nu}_{aR}^c) \begin{pmatrix} 0 & m_{ab} \\ m_{ba} & M_{ab} \end{pmatrix} \begin{pmatrix} \nu_{bL}^c \\ \nu_{bR} \end{pmatrix} + H.c., \end{aligned} \quad (12)$$

where

$$m_{ab} = -h_{ab}^\nu \frac{v}{\sqrt{2}}, \quad M_{ab} = -f_{ab}^\nu \frac{\Lambda}{\sqrt{2}}. \quad (13)$$

* Corresponding author.

dong.phungvan@phenikaa-uni.edu.vn

† nam.caohoang@phenikaa-uni.edu.vn

‡ loi.duongvan@phenikaa-uni.edu.vn

Hence, the canonical seesaw is naturally recognized in the $U(1)_{B-L}$ gauge completion given that $v \ll \Lambda$ or $m \ll M$, yielding the observed neutrino ($\sim \nu_{aL}$) masses to be

$$m_\nu = -mM^{-1}m^T = h^\nu(f^\nu)^{-1}(h^\nu)^T \frac{v^2}{\sqrt{2}\Lambda}, \quad (14)$$

while the heavy neutrinos ($\sim \nu_{aR}$) obtain large masses at the $B-L$ breaking scale, $M \sim \Lambda$.

The neutrino oscillation data implies $m_\nu \sim 0.1$ eV [1], which leads to

$$\Lambda \sim [(h^\nu)^2/f^\nu]10^{14} \text{ GeV}. \quad (15)$$

The seesaw scale Λ is close to the grand unification scale if $(h^\nu)^2/f^\nu \sim 1$. If $(h^\nu)^2/f^\nu$ is sufficiently small, say $f^\nu \sim 1$ and $h^\nu \sim 10^{-5.5}-10^{-5}$ proportional to the electron Yukawa coupling, we derive $\Lambda \sim 1-10$ TeV, in agreement to the collider bounds [1].

All the above results have been established in the literature. However, a proper realization of residual gauge symmetry of $B-L$ and its implication for dark matter have not emerged yet. Let us call the reader's attention to previous works [15–24] relevant to this proposal.

Residual symmetry and dark matter. The symmetry breaking scheme is obtained as

$$\begin{aligned} & SU(3)_C \otimes SU(2)_L \otimes U(1)_Y \otimes U(1)_{B-L} \\ & \quad \downarrow \Lambda \\ & SU(3)_C \otimes SU(2)_L \otimes U(1)_Y \otimes R \\ & \quad \downarrow v \\ & SU(3)_C \otimes U(1)_Q \otimes R \end{aligned}$$

Here the electric charge is related to the isospin and hypercharge as $Q = T_3 + Y$. R is a residual symmetry of $U(1)_{B-L}$ that conserves the χ vacuum, although this vacuum $\langle \chi \rangle = \Lambda/\sqrt{2} \neq 0$ breaks $B-L$ by two unit. As being a $U(1)_{B-L}$ transformation, $R = e^{i\alpha(B-L)}$ where α is a transforming parameter. The vacuum conservation condition $R\langle \chi \rangle = \langle \chi \rangle$ leads to $e^{i\alpha(2)} = 1$, or equivalently $\alpha = k\pi$ for k integer. Hence, the residual symmetry is

$$R = e^{ik\pi(B-L)} = (e^{i\pi(B-L)})^k. \quad (16)$$

It is noted that the transformation with k is conjugated to that with $-k$, i.e. $R^\dagger = (e^{i\pi(B-L)})^{-k} = R^{-1}$.

Field	(ν, e)	(u, d)	(ϕ, χ, A)
R	$(-1)^{-k}$	$e^{ik\pi/3}$	1

TABLE I. R values of leptons, quarks, and bosons, where the generation and left/right chirality indices are omitted since the relevant fields have the same R value.

Let us commonly denote A to be the gauge fields associated with the gauge symmetry in (1). The R values of all fields are collected in Table I. From this table, we derive that $R = 1$ for the minimal value of $|k| = 6$ and

for every field, except the identity $k = 0$. Hence, the residual symmetry R is automorphic to

$$Z_6 = \{1, p, p^2, p^3, p^4, p^5\}, \quad (17)$$

where $p \equiv e^{i\pi(B-L)}$ and $p^6 = 1$. Further, we factorize

$$Z_6 = Z_2 \otimes Z_3, \quad (18)$$

where

$$Z_2 = \{1, p^3\} \quad (19)$$

is the invariant (or normal) subgroup of Z_6 , while

$$Z_3 = Z_6/Z_2 = \{Z_2, \{p, p^4\}, \{p^2, p^5\}\} \quad (20)$$

is the quotient group of Z_6 by Z_2 . Thus, the theory automatically conserves both residual symmetries Z_2 and Z_3 after symmetry breaking.

Field	(ν, e)	(u, d)	(ϕ, χ, A)
1	1	1	1
p^3	-1	-1	1
Z_2	$\underline{1}'_2$	$\underline{1}'_2$	$\underline{1}_2$
p	-1	$-w^2$	1
p^4	1	w^2	1
p^2	1	w	1
p^5	-1	$-w$	1
Z_3	$\underline{1}_3$	$\underline{1}'_3$	$\underline{1}''_3$

TABLE II. Field representations under the residual symmetry $R = Z_2 \otimes Z_3$.

We affix the subscripts $_{2,3}$ to a N -dimensional representation \underline{N} if it is viable, say $\underline{N}_{2,3}$, in order to indicate to those of $Z_{2,3}$, respectively. The field representations under Z_2 and Z_3 are computed in Table II, where $w \equiv e^{i2\pi/3}$ is the cube root of unity. Here note that Z_2 has two (1-dimensional) irreducible representations, $\underline{1}_2$ according to $p^3 = 1$ and $\underline{1}'_2$ according to $p^3 = -1$, whereas Z_3 has three (1-dimensional) irreducible representations, $\underline{1}_3$ according to $(p^2, p^5) = (1, 1)$ or $(1, -1)$, $\underline{1}'_3$ according to $(p^2, p^5) = (w, w)$ or $(w, -w)$, and $\underline{1}''_3$ according to $(p^2, p^5) = (w^2, w^2)$ or $(w^2, -w^2)$, which are independent of p^3 values, 1 or -1 , that identify Z_6 elements in a coset of the quotient group, respectively.¹ The representation $\underline{1}''_3$ is not presented for the existing fields, but the antiquarks (u^c, d^c) belong to $\underline{1}''_3$ under Z_3 .

For brevity, the quotient group can be defined as

$$Z_3 = \{[1], [p^2], [p^4]\}, \quad (21)$$

where each (coset) element $[x]$ consists of two elements of Z_6 , the characteristic x and the other p^3x , as multiplied

¹ The nontrivial representations of Z_3 obey $\underline{1}'_3 \otimes \underline{1}''_3 = \underline{1}_3$, $(\underline{1}'_3)^3 = (\underline{1}''_3)^3 = \underline{1}_3$, $(\underline{1}'_3)^* = \underline{1}''_3 = (\underline{1}'_3)^2$, and $(\underline{1}''_3)^* = \underline{1}'_3 = (\underline{1}''_3)^2$, whereas that of Z_2 satisfies $(\underline{1}'_2)^2 = \underline{1}_2$ and $(\underline{1}'_2)^* = \underline{1}'_2$.

by p^3 . Hence, $[1] = [p^3] = Z_2$, $[p] = [p^4] = \{p, p^4\}$, and $[p^2] = [p^5] = \{p^2, p^5\}$. Because of $[p^4] = [p^2]^2 = [p^2]^*$, the Z_3 group is completely generated by

$$[p^2] = [e^{i2\pi(B-L)}] = [w^{3(B-L)}]. \quad (22)$$

That said, the Z_3 irreducible representations $\underline{1}_3$, $\underline{1}'_3$, and $\underline{1}''_3$ are simply determined by $[p^2] = [1] \rightarrow 1$, $[p^2] = [w] \rightarrow w$, and $[p^2] = [w^2] \rightarrow w^2$, respectively. Here, the intermediate Z_6 representations $[r]$ consists of r and $\pm r$ as multiplied by $p^3 = \pm 1$ respectively, which are homomorphic to that of Z_3 , $[r] = \{r, \pm r\} \rightarrow r$.

Since the spin parity $P_S = (-1)^{2s}$ is always conserved by the Lorentz symmetry, we can conveniently multiply the residual symmetry $R = Z_2 \otimes Z_3$ with spin-parity group $S = \{1, P_S\}$ to perform

$$R \rightarrow R \otimes S = (Z_2 \otimes S) \otimes Z_3, \quad (23)$$

where Z_3 is retained as the quotient group. The new invariant subgroup $Z_2 \otimes S$ defines a matter parity

$$P_M = p^3 \times P_S = (-1)^{3(B-L)+2s}, \quad (24)$$

analogous to the R -parity in supersymmetry.

Because of $P_M^2 = 1$, we have $P = \{1, P_M\}$ to be a group of matter-parity symmetry by itself, which is an invariant subgroup of $Z_2 \otimes S$. Therefore, we factorize

$$R \otimes S = [(Z_2 \otimes S)/P] \otimes P \otimes Z_3. \quad (25)$$

Here $(Z_2 \otimes S)/P = \{P, \{p^3, P_S\}\}$ is conserved, if P_M is conserved. Therefore, instead of $R \otimes S$, we can consider an alternative residual symmetry which is contained in

$$R \otimes S \supset P \otimes Z_3, \quad (26)$$

where the quotient group $(Z_2 \otimes S)/P$ is neglected, since the theory automatically preserves it. Of course, the theory conserves both P and Z_3 , under which the representations under these groups are given in Table III, in which the subscript P indicates to the representations of the matter parity group (P).

Field	(ν, e)	(u, d)	(ϕ, χ, A)
P_M	1	1	1
P	$\underline{1}_P$	$\underline{1}_P$	$\underline{1}_P$
$[p^2]$	1	w	1
Z_3	$\underline{1}_3$	$\underline{1}'_3$	$\underline{1}_3$

TABLE III. Field representations under the alternative residual symmetry $P \otimes Z_3$, where note that the matter parity group P is isomorphic to a Z_2 group generated by P_M , while the quotient group Z_3 is generated by $[p^2]$.

Hence, the model provides a natural stability mechanism for two-component dark matter, in which a dark matter component transforms nontrivially under the matter parity group $P \cong Z_2$ [which should not be confused with the first Z_2 in (19)], i.e. in $\underline{1}'_P$ of P characterized by $P_M = -1$, while the remaining dark matter component transforms nontrivially under the quotient group

Z_3 , i.e. in $\underline{1}'_3$ or $\underline{1}''_3$ of Z_3 characterized by $[p^2] = [w] \rightarrow w$ or $[p^2] = [w^2] \rightarrow w^2$, respectively.

First, to ensure the residual symmetry Z_6 , i.e. $p^6 = \exp[i6\pi(B-L)] = 1$, every dark field should possess a $B-L$ charge, such that $3(B-L)$ is integer. Thus, $[p^2]$ is nontrivial if and only if

$$B-L = \pm \frac{1}{3} + n_1 = \pm \frac{1}{3}, \pm \frac{2}{3}, \pm \frac{4}{3}, \pm \frac{5}{3}, \dots$$

for a generic field. Moreover, P_M is odd if and only if

$$B-L = \frac{1+2n_2}{3} = \pm \frac{1}{3}, \pm 1, \pm \frac{5}{3}, \pm \frac{7}{3}, \dots$$

for bosonic field, and

$$B-L = \frac{2n_3}{3} = 0, \pm \frac{2}{3}, \pm \frac{4}{3}, \pm 2, \dots$$

for fermionic field. The charge parameters $n_{1,2,3}$ are arbitrarily integer. Thus, $B-L$ is quantized with basic periods 1 and $2/3$ resulting from cyclic property of the residual symmetries Z_3 and P , respectively. Additionally, the opposite signs indicate that a field and its conjugation belong to the same kind of dark matter, i.e., nontrivial under Z_3 , P , or both.

To find the minimal realistic setup of two-component dark matter, we demand that the dark sector contains spin-0 bosonic and/or spin-1/2 fermionic fields, transforming as standard model singlets. Additionally, the three kinds of dark fields, P , Z_3 , and both, each have a field, called F_1 , F_2 , and Φ , respectively, where $F_1 \sim (-1, 1)$, $F_2 \sim (1, w/w^2)$, and $\Phi \sim (-1, w/w^2)$ given in terms of $(P_M, [p^2])$ nontrivially transform under P , Z_3 , and both, respectively. Hence their $B-L$ charge is de-

Field	Scalar	Fermion
$[B-L](F_1)$	$1+2n_1$	$2n_1$
$[B-L](F_2)$	$\pm \frac{2}{3} + 2n_2$	$\pm \frac{1}{3} + 2n_2$
$[B-L](\Phi)$	$\pm \frac{2}{3} + 2n_3$	$\pm \frac{1}{3} + 2n_3$

TABLE IV. $B-L$ charge of the dark field kinds that depends on which statistics they obey.

termined in Table IV dependent on which type, either a scalar or a fermion, they are.² Obviously, such a dark field can possess a minimal $B-L$ charge, while its real $B-L$ charge is obtained by the cyclic property. Therefore, F_1 has either $B-L = 0$ as a fermion or ± 1 as a scalar, F_2 has either $B-L = \pm 1/3$ as a fermion or $\pm 2/3$ as a scalar, and Φ has either $B-L = \pm 1/3$ as a scalar or $\pm 2/3$ as a fermion. Among these solutions

² There possibly exist renormalizable couplings of χ to dark fields, such as χF_1^2 , χF_2^3 , $\chi F_1 F_2 \Phi$, and $\chi F_2 \Phi^2$, with appropriate $B-L$ charges, besides the usual ones $(\chi^* \chi)(X^* X)$ for $X = F_1, F_2, \Phi$, given that all the dark fields are scalar.

based upon $P \otimes Z_3$, let us assume the simplest (i.e. most minimal $B - L$) dark matter candidates, as summarized in Table V. Note that the $B - L$ charge of each dark field can deviate from the supplied value by an arbitrary even number—the common multiple of the basic 1 and $2/3$ periods—that necessarily does not change the P, Z_3 representations of the field.³ Here, F and Φ mean fermion and scalar dark fields, respectively. Further, we assume the net mass of F_1 and F_2 is smaller than that of Φ . In this setup, there is no coupling of a χ to two dark fields, because of the Lorentz and $U(1)_{B-L}$ invariance.

Field	P_M	P	$[p^2]$	Z_3
$F_1 \sim (1, 1, 0, 0)$	-1	$\underline{1}'_P$	1	$\underline{1}_3$
$F_2 \sim (1, 1, 0, 1/3)$	1	$\underline{1}_P$	w	$\underline{1}'_3$
$\Phi \sim (1, 1, 0, -1/3)$	-1	$\underline{1}'_P$	w^2	$\underline{1}_3$

TABLE V. Simplest dark matter candidates implied by the residual symmetry $P \otimes Z_3$, where the P and Z_3 representations are determined by the matter parity P_M and the quotient generator $[p^2]$, respectively.

The dark matter component stabilized by P (i.e., F_1) can have an arbitrary mass. This is also valid for the dark matter component stabilized by Z_3 (i.e., F_2), despite the fact that this F_2 component may be heavier than the light quarks u, d . Notice that, since all F_2, u , and d transform nontrivially under Z_3 , this symmetry by itself does not prevent F_2 from decay to quarks. However, when Z_3 is combined with $SU(3)_C$, the F_2 stability is ensured. Prove: Since the Z_3 dark matter component is color neutral, it cannot decay to any colored final state, such as those that include single quarks, because of the color conservation. The $SU(3)_C$ conservation requires a color-neutral final state if it results from a dark matter decay, by assumption. Obviously, this color-neutral final state if constructed from quarks must include only combinations of $q^c q$ and/or qqq (and/or their conjugation). It follows that the final state is invariant (i.e. singlet) under Z_3 too. Because of the Z_3 conservation, such a final state cannot be the product of any Z_3 dark matter decay, which leads to a contradiction. In other words, the $SU(3)_C$ and Z_3 symmetries jointly suppress the decay of Z_3 dark matter component (i.e. stabilized), even if this component has a mass larger than that of quark.

With this proposal, we have the novel, simplest model for two-component dark matter based upon F_1 and F_2 self-interacting through a heavier dark field Φ , which is of course implied by the residual symmetry $P \otimes Z_3$, thus the canonical seesaw. [We can have other scenarios for two-component dark matter, if either the alternative solutions of $F_{1,2}, \Phi$ or more dark fields are introduced and that a coupling of χ to two dark fields may arise. But

they are complicated and suppressed.] Notice that since $F_{1,2}$ and Φ are the standard model singlets, the $U(1)_{B-L}$ dynamics is crucially/sufficiently governing the dark matter observables, besides the known consequences of neutrino mass and baryon asymmetry [25].

Seesaw implication for the XENON1T excess. The XENON1T experiment has recently reported an excess in electronic recoil energy ranging from 1 to 7 keV, peaked around 2.4 keV, having a local statistical significance above 3σ [14]. Such signal of electron recoils seems to reveal the existence of a structured dark sector [26–60].⁴ Indeed, the authors in [27] first showed that in order to fit the excess, the dark matter component that scatters off electrons should be fast moving $v_2 \sim 0.03$ – 0.25 for the dark matter mass $m_2 \sim 0.1$ MeV to 10 GeV, which exceeds the velocity of cold dark matter $v_1 \sim 10^{-3}$.

This fast dark matter component (F_2) may be generated locally as a boosted dark matter from the annihilation or semi-annihilation of the heavier dark matter component (F_1), which is nicely implicated by our model. As a matter of fact, the heavier component with the quantum numbers $F_1 \sim (1, 1, 0, 0)$ interacting with normal matter only via gravity would dominate the cold dark matter, set by its annihilation or co-annihilation to the lighter dark matter component F_2 through the dark matter self-interaction, $\bar{F}_1 F_2 \Phi$ plus its conjugation. The lighter component F_2 sub-dominates the dark matter abundance, since it strongly couples to the Z' portal which is totally annihilated before freezeout.

The relevant Lagrangian terms are

$$\begin{aligned} \mathcal{L} \supset & \bar{F}_1 (i\gamma^\mu \partial_\mu - m_1) F_1 + \bar{F}_2 (i\gamma^\mu D_\mu - m_2) F_2 \\ & + [(D^\mu \Phi)^\dagger (D_\mu \Phi) - m_0^2 \Phi^\dagger \Phi] + \bar{e} (i\gamma^\mu D_\mu - m_e) e \\ & + (h \bar{F}_1 F_2 \Phi + H.c.), \end{aligned} \quad (27)$$

where $D_\mu = \partial_\mu + ig_{B-L}(B-L)Z'_\mu$ and the dark matter masses obey $m_0 > m_1 + m_2$ and $m_1 > m_2$. Since the $B - L$ charge of F_1 is fixed as $B - L = 0$, the remaining dark fields can possess more general $B - L$ charges,

$$F_2 \sim (1, 1, 0, 1/3 + 2n), \quad \Phi \sim (1, 1, 0, -1/3 - 2n), \quad (28)$$

for $n = 0, \pm 1, \pm 2, \dots$, as mentioned.

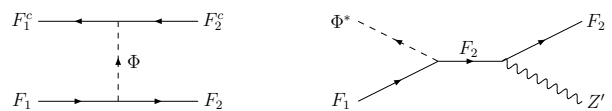


FIG. 1. Annihilation (left) and co-annihilation (right) processes of F_1 that set the cold dark matter density.

The relic density of F_1 is governed by Feynman diagrams in Fig. 1. The co-annihilation process is only

³ The actual $B - L$ charges of the dark fields would be phenomenologically determined.

⁴ For other interpretations, see [61–66], for instance.

enhanced when the masses of F_1 and Φ are highly degenerate. However, this work signifies $m_0 > m_1 + m_2 \sim 2m_1$ such that the co-annihilation contribution is negligible, where notice that $m_2 \sim m_1$ is used, since F_2 is mildly boosted responsible for the XENON1T excess. Hence, the dark matter abundance is given by the F_1 annihilation in the left diagram.

Applying the Feynman rules, we obtain the thermal average cross-section times relative velocity as

$$\langle \sigma v_{\text{rel}} \rangle \simeq \frac{|h|^4 (m_1 + m_2)^2}{8\pi m_0^4} \left(1 - \frac{m_2^2}{m_1^2}\right)^{1/2}, \quad (29)$$

which relates to the F_1 abundance, $\Omega h^2 \simeq 0.1 \text{ pb}/\langle \sigma v_{\text{rel}} \rangle$, where h is the reduced Hubble parameter without confusion. Using the experimental data $\Omega h^2 \simeq 0.12$ [1] and the Lorentz boost by the left diagram $\gamma_2 = m_1/m_2 = (1 - v_2^2)^{-1/2} \approx 1$, i.e. $m_1 \approx m_2$, we get the constraint of the dark matter self-coupling to be

$$|h| \simeq 7 \times 10^{-4} \left(\frac{m_0}{2m_1}\right) \left(\frac{m_1}{1 \text{ MeV}}\right)^{1/2} \left(\frac{\delta m^2}{m_1^2}\right)^{-1/8}, \quad (30)$$

which translates to $|h| \gtrsim 10^{-3}$, because of $m_0 \gtrsim 2m_1$, $m_1 \gtrsim 1 \text{ MeV}$, and $\delta m^2/m_1^2 = (m_1^2 - m_2^2)/m_1^2 \simeq v_2^2 \sim 1\%$ as shown below. Since the F_1 dark matter is thermally generated, its mass has been assumed to be larger than the BBN and CMB bounds $\sim 1 \text{ MeV}$ which are hereafter taken as the electron mass, i.e. $m_1 > m_e$ [67].

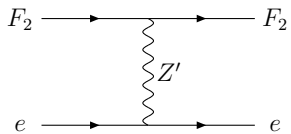


FIG. 2. Scattering process of the boosted dark matter F_2 with electrons in the XENON1T experiment.

Of course, at present, F_2 is locally generated by the left diagram in Fig. 1 which subsequently scatters off electrons in the XENON1T experiment through the diagram in Fig. 2. The recoil energy, deposited by the F_2 -electron scattering, required to fit the excess is few keV, i.e. $E_R \sim 2.4 \text{ keV}$. In this model, since the F_2 mass satisfies $m_2 \approx m_1 > m_e$, the electronic recoil energy is estimated as $E_R = E_{e'} - E_e = 2\mu v_{\text{rel}} v_{\text{cm}} < 2m_e v_2^2$, where the incoming velocities of F_2 and e , called v_2 and v_e respectively, are assumed to be parallel, $\mu = m_2 m_e / (m_2 + m_e)$ is the reduced mass, $v_{\text{rel}} = v_2 - v_e$ is the relative velocity, and $v_{\text{cm}} = (m_2 v_2 + m_e v_e) / (m_2 + m_e)$ is the center-of-mass velocity. Thus, the recoil energy is comparable to the observed value if F_2 is boosted with a velocity $v_2 \sim 0.1$, in agreement to the best fit in [27]. This yields a transferred momentum $q = -E_R / v_{\text{cm}}$, such that $|q| \sim 40 \text{ keV}$. In the limit of mediator mass $m_{Z'}$ to be much larger than the momentum transfer, $m_{Z'} \gg |q|$, the F_2 -electron scat-

tering cross-section can be written as [68]

$$\sigma_e = \frac{g_{B-L}^4 (1/3 + 2n)^2 m_e^2}{\pi m_{Z'}^4}. \quad (31)$$

This leads to the number of the signal events as related to the scattering cross-section by [35, 69]

$$\frac{N_{\text{sig}}}{100} = \frac{16\sigma_e}{3 \text{ pb}} \left(\frac{1 \text{ MeV}}{m_1}\right)^2. \quad (32)$$

The mass of Z' boson is $m_{Z'} = 2g_{B-L}\Lambda$, where the contribution of the kinetic mixing effect between the $U(1)_Y$ and $U(1)_{B-L}$ gauge bosons is radically small and neglected [1]. Therefore, the scattering cross-section becomes $\sigma_e = (1/3 + 2n)^2 m_e^2 / (16\pi\Lambda^4)$, which does not explicitly depend on the Z' mass, $m_{Z'}$, and the Z' coupling, g_{B-L} , but on the $B-L$ breaking scale $\Lambda = m_{Z'} / 2g_{B-L}$, governed by the ratio of the Z' mass to the Z' coupling. Additionally, the new observation is that the cross-section is significantly enhanced by the $B-L$ charge of F_2 dark matter as multiplied by n^2 as this charge is large, but it is suppressed by the new physics scale to be $1/\Lambda^4$. Correspondingly, the event number is proportional to $N_{\text{sig}}/100 \sim (10^{-5}n)^2 (m_e/m_1)^2 (\text{TeV}/\Lambda)^4$, as enhanced by n^2 , but suppressed by $1/m_1^2 \times 1/\Lambda^4$.

The viable regime of the dark matter charge and the new physics scale is determined by making a contour of $N_{\text{sig}}/100 = 1$ from (32) as implied by the XENON1T experiment to be a function of (n, Λ) as in Fig. 3 upper panel, taking the lower mass limit for thermal dark matter $m_1 = m_e \simeq 0.51 \text{ MeV}$, where the collider bound $\Lambda = 3 \text{ TeV}$ is shown (cf. Appendix A), as well as noting that the thermal dark matter excluded region corresponds to $m_1 < m_e$. On the other hand, the enhancement of the event number in terms of the dark matter charge is illustrated in Fig. 3 lower panel, taking into account some allowed values of the dark matter mass and the new physics scale from the above regime:

$$(m_1, \Lambda) = (0.51, 3), (0.51, 5), (5, 3), (5, 5), \quad (33)$$

in (MeV, TeV), respectively.

Remarks are in order

1. From the figure, the dark matter charge has a lower limit to be large, required in order to explain the number of the signal events, $N_{\text{sig}}/100 = 1$, i.e.

$$|1 + 6n| \simeq 915.15 \frac{m_1 \Lambda^2}{\text{GeV}^3}, \quad (34)$$

since both Λ and m_1 have a lower bound, $\Lambda = 3 \text{ TeV}$ and $m_1 = m_e$, implying

$$|n| \simeq 0.7 \times 10^6. \quad (35)$$

This coincides with the n value in Fig. 3 at which the red line intersects either $\Lambda = 3 \text{ TeV}$ in the upper panel or $N_{\text{sig}}/100 = 1$ in the lower panel.

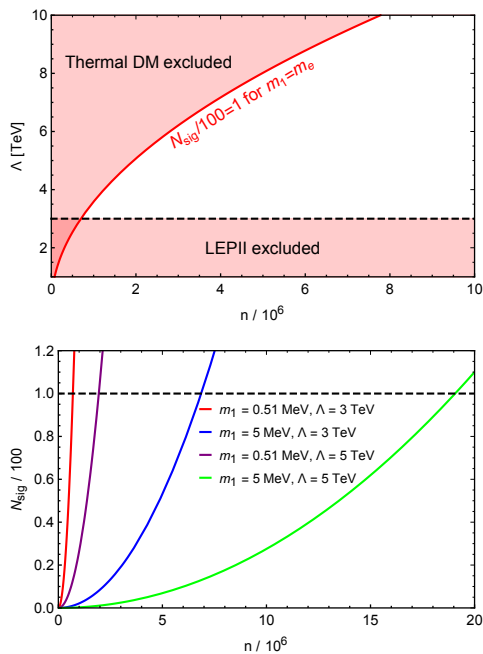


FIG. 3. Upper panel: Allowed (white) region of (n, Λ) determined by (i) contour of $N_{\text{sig}}/100 = 1$ as a function of (n, Λ) according to the WIMP mass limit $m_1 = m_e$ and (ii) inclusion of the collider constraint on Λ . Lower panel: Number of the signal events, $N_{\text{sig}}/100$, significantly enhanced by the fast dark matter charge for the reference values of the thermal dark matter mass and the new physics scale.

- Also from the figure, the model can generally maintain the excess in XENON1T with a stronger $B-L$ breaking scale and/or larger dark matter mass, but this requires the minimum value of n to be correspondingly enhanced, which is indeed bigger than that in (35) by factors $(m_1/m_e)(\Lambda/3\text{TeV})^2$. For instance, we obtain

$$|n| \simeq 1.94 \times 10^6, 6.86 \times 10^6, 1.9 \times 10^7, \quad (36)$$

according to the last three pairs of (m_1, Λ) in (33), which can be seen in Fig. 3 lower panel when the relevant curves intersect the dashed line.

The nature of a large $U(1)$ charge and the behavior of its coupling are explained in Appendix B. From the remark 1 and 2, such a minimum value of n would translate to an upper bound for g_{B-L} and $m_{Z'}$, as shown below.

- Obviously, the model with $n = 0$ fails to account for the excess, unless the kinetic mixing and g_{B-L} fine-tuning to unnaturally small values is imposed, which is not interpreted in this work.

Applying the criteria in Appendix B to $U(1)_{B-L}$, we approximate $b_{B-L} \simeq -(5/3)(1/3 + 2n)^2$, thus

$$\mu \partial g'_{B-L} / \partial \mu \simeq (5/48\pi^2) g_{B-L}^3, \quad (37)$$

which yields that $g'_{B-L} \equiv |1/3 + 2n|g_{B-L}$ slides similarly to the usual one. The solution is

$$\alpha'^{-1} = \alpha_G'^{-1} - (5/6\pi) \ln(\mu/\mu_G), \quad (38)$$

where $\alpha' \equiv g_{B-L}^2/4\pi$ and a subscript G referring to that of the GUT (the Planck regime may be chosen, but not necessary). Further, one demands a perturbative limit for the $U(1)_{B-L}$ gauge interaction at the GUT scale, i.e. $\alpha'_G \simeq 1$ at $\mu_G \sim 10^{16}$ GeV, which also necessarily prevents a proton decay since it occurs only via a GUT breakdown. This leads to $\alpha' \simeq 0.08$ at the scale of interest, $\mu \sim 1$ MeV.⁵ Thus, we get

$$g'_{B-L} = |1/3 + 2n|g_{B-L} \simeq 1. \quad (39)$$

According to the values of n in (35) and (36), the relation (39) implies upper bounds for

$$g_{B-L} \simeq \frac{0.5}{n} \simeq 7.1 \times 10^{-7}, 2.6 \times 10^{-7}, \\ 7.2 \times 10^{-8}, 2.6 \times 10^{-8}, \quad (40)$$

respectively. With the aid of (34) and (39), the Z' mass is rewritten as

$$m_{Z'} \simeq 3.62 \times 10^3 (g_{B-L}/m_1)^{1/2} \text{MeV}^{3/2}. \quad (41)$$

Corresponding to the above values of (g_{B-L}, m_1) , the Z' mass is bounded, respectively, by

$$m_{Z'} \simeq 4.3, 2.6, 0.43, 0.26 \text{ MeV}. \quad (42)$$

Notice that if (m_1, Λ) are higher than those in (33), the Z' coupling and mass get more restricted.

Since the Z' mass is radically low, the constraints from low energy experiments apply. Because of the conditions for $m_{Z'}$ in (C2) as well as $m_2 < m_0$, the Z' boson cannot decay invisibly to any dark field, $\text{Br}(Z' \rightarrow F_2^c F_2) = \text{Br}(Z' \rightarrow \Phi^* \Phi) = 0$, and obviously $\text{Br}(Z' \rightarrow F_1^c F_1) = 0$. Hence, Z' may only decay to the neutrinos $Z' \rightarrow \nu_L^c \nu_L$ and charged leptons $Z' \rightarrow e^+ e^-$ if $m_{Z'} > 2m_e$, being the same with the usual $U(1)_{B-L}$ model, studied in [70–76]. That said, the $U(1)_{B-L}$ gauge coupling is strongly constrained by the beam dump experiments to be roundly $g_{B-L} \sim 10^{-8}$ for $m_{Z'} = 1\text{--}10$ MeV (cf. the figures 5 and 13 of [73] and [74], respectively). Such bound excludes the values of g_{B-L} in (40) that correspond to $m_{Z'} > 2m_e \simeq 1$ MeV given in (42). However, the bound does not apply to g_{B-L} that reduces $m_{Z'}$ below 1 MeV, since the detectors in such experiments are only sensitive to the signal of $Z' \rightarrow e^+ e^-$ decay. Precisely, with the aid of (41), the surviving condition $m_{Z'} < 1$ MeV leads to

$$g_{B-L} < 3.9 \times 10^{-8} (m_1/m_e). \quad (43)$$

⁵ Generally, the physical processes relevant to the gauge interactions of F_2 and Φ are determined by α' , thus are perturbative, since α' decreases below 1 when the energy scale decreases below the GUT scale.

This regime excludes the processes (i) in App. C that set the F_2 density at Z' resonance $m_{Z'} = 2m_2 > 1$ MeV, despite $\Omega_{F_2} h^2 \sim (4m_2^2 - m_{Z'}^2)^2 / (m_2^2 m_{Z'}^2)$ tending to zero as desirable, where it yields $g_{B-L} > 4 \times 10^{-8}$ in tension with the bound $g_{B-L} \sim 10^{-8}$.

Below $m_{Z'} = 1$ MeV, the model is constrained by several experiments: The neutrino-electron scattering exchanged by Z' fully studied in [71] using the measurements from Borexino [77], Texono [78], and Charm-II ($\bar{\nu}_\mu$) [79, 80]; The energy loss, carried by Z' , of the horizontal branch (HB) stars [81] and the supernova 1987A (SN1987A) [82, 83]. Including the beam dump experiments given by the darkcast package [73] using the measurements from E137 [84], ν -CAL I [85, 86], Orsay [87], and E141 [88], all the relevant experimental constraints and the model prediction from (41) are plotted in Figure 4. Hence, $m_1 = 165$ MeV is the upper limit of dark

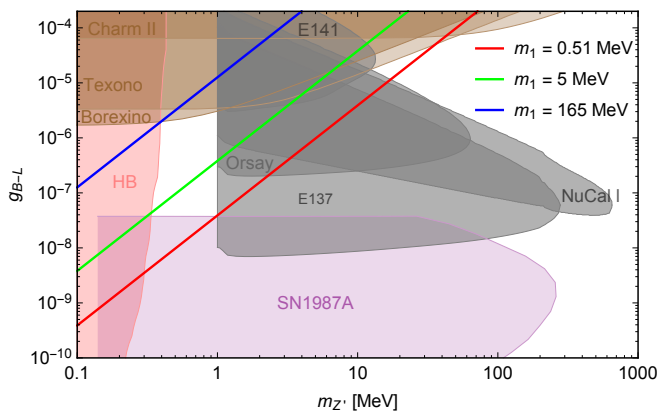


FIG. 4. Theoretical prediction (41) for dark matter mass $m_1 = 0.51, 5,$ and 165 MeV, where the relevant strongest experimental constraints (the color regions denote excluded parameter space according to each experiment) have been adapted from [73] for the beam dump (E137, ν -CAL I, Orsay, and E141), [71] for the neutrino-electron scattering (Borexino, Texono, and Charm II with $\bar{\nu}_\mu$), [72] for the HB stars (extracted from [81]), and [70] for the SN1987A (translated from [82]), where $m_1 = 165$ MeV was chosen so that the theoretical prediction intersects the HB and Borexino bounds.

matter mass determined by the HB and Borexino bounds, while it is confidently that $m_1 \simeq m_e \simeq 0.51$ MeV is the lower limit of dark matter mass at which the theory approximately coincides with the E137 and SN1987A bounds, that is

$$0.51 \text{ MeV} < m_1 < 165 \text{ MeV}. \quad (44)$$

Further, our model predicts

$$0.34 \text{ MeV} < m_{Z'} < 1 \text{ MeV}, \quad (45)$$

limited by the HB and the beam dump insensitivity, and

$$3.8 \times 10^{-8} < g_{B-L} < 2.9 \times 10^{-6}, \quad (46)$$

bounded by the SN1987A and the Borexino, respectively. Notice that the region close to the top of Fig. 4, that is

bounded by the red line $m_1 = 0.51$ MeV and allowed by the Texono and Orsay experiments, is excluded by the XENON1T, since $m_{Z'} \leq 4.3$ MeV.

Conclusion. We have discovered a seminal result of the seesaw mechanism with gauged $B-L$ symmetry, alternative to the known leptogenesis, that it manifestly solves the long-standing issue of structured dark matter. The seesaw scale presents a nontrivial physical vacuum preserving two residual gauge symmetries, relating to the usual matter parity $P_M = (-1)^{3(B-L)+2s}$ and a new Z_3 quotient $[p^2] = [w^{3(B-L)}]$. This yields a two-component dark matter scenario naturally addressing the recent XENON1T excess. The cold dark matter F_1 has $B-L = 0$, while the boosted dark matter F_2 has $B-L$ deviating from $1/3$ by seven order (roundly), and their masses $m_{1,2}$ obey $\text{Max}(m_e, m_{Z'}) < m_1 \approx m_2 < 165$ MeV. The Z' mass and coupling predicted are $0.34 \text{ MeV} < m_{Z'} < 1 \text{ MeV}$ and $3.8 \times 10^{-8} < g_{B-L} < 2.9 \times 10^{-6}$, respectively. If the XENON1T experiment is relaxed, a scheme of two-component dark matter beyond the weak scale is warranted, presented in standard model gauge extensions containing a $B-L$ charge, such as the left-right symmetry and $SO(10)$.

Acknowledgments. This research is funded by Vietnam National Foundation for Science and Technology Development (NAFOSTED) under grant number 103.01-2019.353.

Appendix A: High energy collider constraint

Contribution of Z' to the process $e^+e^- \rightarrow f\bar{f}$, where f is an ordinary fermion, proceeds through the $f\bar{f}$ exchange either by s -channel diagram for $f \neq e$ or by s, t, u -channel diagrams for $f = e$.

If $m_{Z'} < \sqrt{s} = 209$ GeV as in this model, the Z' boson is resonantly produced at the LEP II and the agreement between the LEP II and the standard model indicates that the Z' -fermion couplings are $g_{B-L} \lesssim 10^{-2}$, given that Z' does not decay to the dark fields F_2, Φ [89]. However, when $m_{Z'} > 2m_{F_2, \Phi}$, the decay to the dark fields dominates the Z' width and then the cross-section $\sigma(e^+e^- \rightarrow f\bar{f}) = \sigma(e^+e^- \rightarrow Z')\text{Br}(Z' \rightarrow f\bar{f})$ is strongly suppressed, since $\text{Br}(Z' \rightarrow f\bar{f}) \sim 1/n^2 \ll 1$. This case requiring $g_{B-L}/n \lesssim 10^{-2}$ is obviously satisfied for the n value of interest and g_{B-L} in perturbative regime.

By contrast, if $m_{Z'} > \sqrt{s} = 209$ GeV, the process $e^+e^- \rightarrow f\bar{f}$ receives an off-shell contribution of Z' , best described by the effective interaction,

$$\mathcal{L}_{\text{eff}} \supset \frac{g_{B-L}^2 (B-L)_f}{m_{Z'}^2 - s} (\bar{e}\gamma^\nu e)(\bar{f}\gamma_\nu f). \quad (A1)$$

Considering $f = \mu, \tau$, the LEP II has limited the Z' mass over coupling to be $m_{Z'}/g_{B-L} \geq 6$ TeV, which translates to the breaking scale $\Lambda \geq 3$ TeV [90, 91].

Additionally, the LHC has searched for dilepton signals $pp \rightarrow l\bar{l}$ as mediated by Z' , yielding a mass limit roundly

$m_{Z'} = 4$ TeV for the Z' coupling identical to Z , which converts to a bound for $\Lambda \sim m_{Z'}/2g \sim 3$ TeV, similar to the LEP II [92]. Here Z' does not decay to the dark matter. Otherwise, the cross-section is more suppressed, similar to the LEP II case.

As a matter of fact, Z' cannot decay to the dark fields in this model [cf. (C2)]. The production of mono- X or two- X 's final state (signature) recoils against large missing momentum (or energy) carried by dark matter is insensitive to the LEP II and LHC detectors, because of the suppression $\text{Br}(Z' \rightarrow \text{DM DM}) = 0$.

In short, these experiments give a reference of the new physics scale, say $\Lambda = 3$ TeV, used in the body text.

Appendix B: Nature of $U(1)$ charge and running coupling

In contrast to the non-Abelian charges (e.g., the color and the weak isospin) that are constrained by the non-Abelian nature of a Lie algebra, $[T_j, T_k] = if_{jkl}T_l$ with $\text{Tr}(T_j T_k) \sim \delta_{jk}$, the Abelian charges including electric charge are completely arbitrary, often chosen to describe observed charge values, while do not explain them.

Indeed, the Hamiltonian of a $U(1)_X$ gauge theory preserves a scaling symmetry, $g_X \rightarrow g'_X = g_X/\lambda$ and $X \rightarrow X' = \lambda X$, where g'_X and X' are the respective coupling and charge after the transformation. We can work in a basis that g_X is small, while X is large, which leaves the physics unchanged.

For instance, the running of g_X with renormalization scale μ satisfies the RG equation,

$$\mu dg_X/\partial\mu = \beta(g_X) = -(g_X^3/16\pi^2)b_X, \quad (\text{B1})$$

where the beta function at 1-loop level is given by

$$b_X = -\frac{2}{3} \sum_L X_L^2 - \frac{2}{3} \sum_R X_R^2 - \frac{1}{3} \sum_S X_S^2 \quad (\text{B2})$$

as summed over the left/right chiral fermion and scalar fields, respectively. The equation (B1) conserves the above scaling symmetry as a result, implying that a theory with large X behaves similarly to the usual ones.

A character of the $U(1)$ theory is that the function $b_X < 0$ for every X -charge. Therefore, its gauge coupling g_X decreases when the energy scale μ decreases. Given

that the theory is definite at a GUT or Planck scale, i.e. $g_X X \sim 1$, it must properly work to be perturbative and predictive below such large scale.

Appendix C: Condition of vanished F_2 density

Last, but not least, it is verified that the F_2 relic density should be negligible. In the early universe, the dark field F_2 might completely annihilate to (i) the standard model particles such as $F_2^c F_2 \rightarrow l^+ l^-, \nu_L^c \nu_L$ via the (s -channel) Z' portal or to (ii) the new gauge boson $F_2^c F_2 \rightarrow Z' Z'$ via t - and u -channel diagrams mediated by just F_2 , if kinetically allowed.

If $m_2 < m_{Z'}$, the annihilation proceeds through the first processes (i), yielding the cross-sections

$$\langle\sigma v_{\text{rel}}\rangle_{F_2^c F_2 \rightarrow e^+ e^-, \nu_L^c \nu_L} \sim \begin{cases} \left(\frac{m_{Z'}}{2 \text{ MeV}}\right)^4 \text{ pb,} & \text{if } m_2 > \frac{1}{2} m_{Z'} \\ \left(\frac{m_2}{1 \text{ MeV}}\right)^4 \text{ pb,} & \text{if } m_2 < \frac{1}{2} m_{Z'} \end{cases}$$

with the help of (34) as well as $m_1 \approx m_2$, where the resonance $m_2 = \frac{1}{2} m_{Z'}$ need not necessarily be considered since it sets a lowest F_2 relic density. Although one vertex (namely $\bar{F}_2 F_2 Z'$) is enhanced by the coupling strength $g'_{B-L} = |1/3 + 2n|g_{B-L} \simeq 1$, these contributions are only effective if $\text{Min}\{m_2, \frac{1}{2} m_{Z'}\} > 1$ MeV. In this case, since $m_1 \approx m_2 > 1$ MeV, we obtain the Z' mass bound to be $m_{Z'} < 2.2$ MeV due to (41), (39), and (34) for $\Lambda \geq 3$ TeV. That said, the above possibilities give a finite contribution to dark matter, since $\langle\sigma v_{\text{rel}}\rangle_{F_2^c F_2 \rightarrow e^+ e^-, \nu_L^c \nu_L} \sim 1$ pb, except for the resonance regime at which the F_2 density almost vanishes.

By contrast, if $m_2 > m_{Z'}$, the last process (ii) produces a large annihilation cross-section to be

$$\langle\sigma v_{\text{rel}}\rangle_{F_2^c F_2 \rightarrow Z' Z'} \simeq \frac{|M|^2}{16\pi s} \gg 1 \text{ pb}, \quad (\text{C1})$$

because the amplitude $M(F_2^c F_2 \rightarrow Z' Z') \simeq 4g_{B-L}^4$ that is induced in the order of unity is strongly enhanced by both the $\bar{F}_2 F_2 Z'$ vertices with the coupling strength $g'_{B-L} = |1/3 + 2n|g_{B-L} \simeq 1$ and that $s \simeq 4m_2^2 < \text{GeV}^2$.

Summarizing all the relevant cross-sections leads to $\Omega_{F_2} h^2 \simeq 0.1 \text{ pb}/\langle\sigma v_{\text{rel}}\rangle_{F_2^c F_2 \rightarrow \text{all}} \ll 0.12$, provided that

$$m_2 > m_{Z'}, \text{ or else } m_2 = \frac{1}{2} m_{Z'}. \quad (\text{C2})$$

-
- [1] PARTICLE DATA GROUP collaboration, *Review of Particle Physics*, *Phys. Rev.* **D98** (2018) 030001.
[2] P. Minkowski, $\mu \rightarrow e\gamma$ at a Rate of One Out of 10^9 Muon Decays?, *Phys. Lett.* **67B** (1977) 421.
[3] M. Gell-Mann, P. Ramond and R. Slansky, *Complex Spinors and Unified Theories*, *Conf. Proc.* **C790927** (1979) 315 [1306.4669].

- [4] T. Yanagida, *Horizontal symmetry and masses of neutrinos*, *Conf. Proc.* **C7902131** (1979) 95.
[5] S. L. Glashow, *The Future of Elementary Particle Physics*, *NATO Sci. Ser. B* **61** (1980) 687.
[6] R. N. Mohapatra and G. Senjanovic, *Neutrino Mass and Spontaneous Parity Violation*, *Phys. Rev. Lett.* **44** (1980) 912.

- [7] R. N. Mohapatra and G. Senjanovic, *Neutrino Masses and Mixings in Gauge Models with Spontaneous Parity Violation*, *Phys. Rev.* **D23** (1981) 165.
- [8] G. Lazarides, Q. Shafi and C. Wetterich, *Proton Lifetime and Fermion Masses in an $SO(10)$ Model*, *Nucl. Phys.* **B181** (1981) 287.
- [9] J. Schechter and J. W. F. Valle, *Neutrino Masses in $SU(2) \times U(1)$ Theories*, *Phys. Rev.* **D22** (1980) 2227.
- [10] J. Schechter and J. W. F. Valle, *Neutrino Decay and Spontaneous Violation of Lepton Number*, *Phys. Rev.* **D25** (1982) 774.
- [11] A. Davidson, *$B - L$ as the fourth color within an $SU(2)_L \times U(1)_R \times U(1)$ model*, *Phys. Rev.* **D20** (1979) 776.
- [12] R. E. Marshak and R. N. Mohapatra, *Quark - Lepton Symmetry and $B-L$ as the $U(1)$ Generator of the Electroweak Symmetry Group*, *Phys. Lett.* **91B** (1980) 222.
- [13] R. N. Mohapatra and R. E. Marshak, *Local $B-L$ Symmetry of Electroweak Interactions, Majorana Neutrinos and Neutron Oscillations*, *Phys. Rev. Lett.* **44** (1980) 1316.
- [14] XENON collaboration, *Excess electronic recoil events in XENON1T*, *Phys. Rev. D* **102** (2020) 072004 [2006.09721].
- [15] L. M. Krauss and F. Wilczek, *Discrete Gauge Symmetry in Continuum Theories*, *Phys. Rev. Lett.* **62** (1989) 1221.
- [16] S. P. Martin, *Some simple criteria for gauged R -parity*, *Phys. Rev. D* **46** (1992) 2769 [hep-ph/9207218].
- [17] B. Batell, *Dark Discrete Gauge Symmetries*, *Phys. Rev. D* **83** (2011) 035006 [1007.0045].
- [18] E. Ma, *Derivation of Dark Matter Parity from Lepton Parity*, *Phys. Rev. Lett.* **115** (2015) 011801 [1502.02200].
- [19] E. Ma, N. Pollard, R. Srivastava and M. Zakeri, *Gauge $B - L$ Model with Residual Z_3 Symmetry*, *Phys. Lett. B* **750** (2015) 135 [1507.03943].
- [20] M. Hirsch, R. Srivastava and J. W. F. Valle, *Can one ever prove that neutrinos are Dirac particles?*, *Phys. Lett. B* **781** (2018) 302 [1711.06181].
- [21] C. Bonilla, S. Centelles-Chuliá, R. Cepedello, E. Peinado and R. Srivastava, *Dark matter stability and Dirac neutrinos using only Standard Model symmetries*, *Phys. Rev. D* **101** (2020) 033011 [1812.01599].
- [22] J. Heeck and W. Rodejohann, *Neutrinoless Quadruple Beta Decay*, *EPL* **103** (2013) 32001 [1306.0580].
- [23] C. Cai, Z. Kang, H.-H. Zhang and Y.-P. Zeng, *Minimal dark matter in $SU(2)_L \times U(1)_Y \times U(1)_{B-L}$* , *Phys. Lett. B* **784** (2018) 385 [1801.05594].
- [24] D. Nanda and D. Borah, *Connecting Light Dirac Neutrinos to a Multi-component Dark Matter Scenario in Gauged $B - L$ Model*, *Eur. Phys. J. C* **80** (2020) 557 [1911.04703].
- [25] M. Fukugita and T. Yanagida, *Baryogenesis Without Grand Unification*, *Phys. Lett.* **B174** (1986) 45.
- [26] F. Takahashi, M. Yamada and W. Yin, *XENON1T Excess from Anomaly-Free Axionlike Dark Matter and Its Implications for Stellar Cooling Anomaly*, *Phys. Rev. Lett.* **125** (2020) 161801 [2006.10035].
- [27] K. Kannike, M. Raidal, H. Veermäe, A. Strumia and D. Teresi, *Dark Matter and the XENON1T electron recoil excess*, *Phys. Rev. D* **102** (2020) 095002 [2006.10735].
- [28] G. Choi, M. Suzuki and T. T. Yanagida, *XENON1T Anomaly and its Implication for Decaying Warm Dark Matter*, 2006.12348.
- [29] J. Buch, M. A. Buen-Abad, J. Fan and J. S. C. Leung, *Galactic Origin of Relativistic Bosons and XENON1T Excess*, 2006.12488.
- [30] Y. Chen, J. Shu, X. Xue, G. Yuan and Q. Yuan, *Sun Heated MeV-scale Dark Matter and the XENON1T Electron Recoil Excess*, 2006.12447.
- [31] N. F. Bell, J. B. Dent, B. Dutta, S. Ghosh, J. Kumar and J. L. Newstead, *Explaining the XENON1T excess with Luminous Dark Matter*, *Phys. Rev. Lett.* **125** (2020) 161803 [2006.12461].
- [32] M. Du, J. Liang, Z. Liu, V. Q. Tran and Y. Xue, *On-shell mediator dark matter models and the Xenon1T excess*, *Chin. Phys. C* **45** (2021) 013114 [2006.11949].
- [33] L. Su, W. Wang, L. Wu, J. M. Yang and B. Zhu, *Atmospheric Dark Matter and Xenon1T Excess*, *Phys. Rev. D* **102** (2020) 115028 [2006.11837].
- [34] K. Harigaya, Y. Nakai and M. Suzuki, *Inelastic Dark Matter Electron Scattering and the XENON1T Excess*, *Phys. Lett. B* **809** (2020) 135729 [2006.11938].
- [35] B. Fornal, P. Sandick, J. Shu, M. Su and Y. Zhao, *Boosted Dark Matter Interpretation of the XENON1T Excess*, *Phys. Rev. Lett.* **125** (2020) 161804 [2006.11264].
- [36] G. Alonso-Álvarez, F. Ertas, J. Jaeckel, F. Kahlhoefer and L. J. Thormaehlen, *Hidden Photon Dark Matter in the Light of XENON1T and Stellar Cooling*, *JCAP* **11** (2020) 029 [2006.11243].
- [37] Y. Jho, J.-C. Park, S. C. Park and P.-Y. Tseng, *Leptonic New Force and Cosmic-ray Boosted Dark Matter for the XENON1T Excess*, *Phys. Lett. B* **811** (2020) 135863 [2006.13910].
- [38] M. Baryakhtar, A. Berlin, H. Liu and N. Weiner, *Electromagnetic Signals of Inelastic Dark Matter Scattering*, 2006.13918.
- [39] I. M. Bloch, A. Caputo, R. Essig, D. Redigolo, M. Sholapurkar and T. Volansky, *Exploring New Physics with $O(\text{keV})$ Electron Recoils in Direct Detection Experiments*, 2006.14521.
- [40] G. Paz, A. A. Petrov, M. Tamaro and J. Zupan, *Shining dark matter in Xenon1T*, 2006.12462.
- [41] Q.-H. Cao, R. Ding and Q.-F. Xiang, *Exploring for sub-MeV Boosted Dark Matter from Xenon Electron Direct Detection*, 2006.12767.
- [42] H. M. Lee, *Exothermic dark matter for XENON1T excess*, *JHEP* **01** (2021) 019 [2006.13183].
- [43] K. Nakayama and Y. Tang, *Gravitational Production of Hidden Photon Dark Matter in Light of the XENON1T Excess*, *Phys. Lett. B* **811** (2020) 135977 [2006.13159].
- [44] R. Primulando, J. Julio and P. Uttayarat, *Collider Constraints on a Dark Matter Interpretation of the XENON1T Excess*, *Eur. Phys. J. C* **80** (2020) 1084 [2006.13161].
- [45] G. B. Gelmini, V. Takhistov and E. Vitagliano, *Scalar direct detection: In-medium effects*, *Phys. Lett. B* **809** (2020) 135779 [2006.13909].
- [46] J. Bramante and N. Song, *Electric But Not Eclectic: Thermal Relic Dark Matter for the XENON1T Excess*, *Phys. Rev. Lett.* **125** (2020) 161805 [2006.14089].
- [47] L. Zu, G.-W. Yuan, L. Feng and Y.-Z. Fan, *Mirror Dark Matter and Electronic Recoil Events in XENON1T*,

- 2006.14577.
- [48] S. Baek, J. Kim and P. Ko, *XENON1T excess in local Z_2 DM models with light dark sector*, *Phys. Lett. B* **810** (2020) 135848 [2006.16876].
- [49] H. Alhazmi, D. Kim, K. Kong, G. Mohlabeng, J.-C. Park and S. Shin, *Implications of the XENON1T Excess on the Dark Matter Interpretation*, 2006.16252.
- [50] W. Chao, Y. Gao and M. j. Jin, *Pseudo-Dirac Dark Matter in XENON1T*, 2006.16145.
- [51] L. Delle Rose, G. Hütsi, C. Marzo and L. Marzola, *Impact of loop-induced processes on the boosted dark matter interpretation of the XENON1T excess*, *JCAP* **02** (2021) 031 [2006.16078].
- [52] P. Ko and Y. Tang, *Semi-annihilating Z_3 dark matter for XENON1T excess*, *Phys. Lett. B* **815** (2021) 136181 [2006.15822].
- [53] H. An and D. Yang, *Direct detection of freeze-in inelastic dark matter*, 2006.15672.
- [54] N. Okada, S. Okada, D. Raut and Q. Shafi, *Dark matter Z' and XENON1T excess from $U(1)_X$ extended standard model*, *Phys. Lett. B* **810** (2020) 135785 [2007.02898].
- [55] D. Choudhury, S. Maharana, D. Sachdeva and V. Sahdev, *Dark matter, muon anomalous magnetic moment, and the XENON1T excess*, *Phys. Rev. D* **103** (2021) 015006 [2007.08205].
- [56] G. Arcadi, A. Bally, F. Goertz, K. Tame-Narvaez, V. Tenorth and S. Vogl, *EFT interpretation of XENON1T electron recoil excess: Neutrinos and dark matter*, *Phys. Rev. D* **103** (2021) 023024 [2007.08500].
- [57] H.-J. He, Y.-C. Wang and J. Zheng, *EFT Approach of Inelastic Dark Matter for Xenon Electron Recoil Detection*, *JCAP* **01** (2021) 042 [2007.04963].
- [58] U. K. Dey, T. N. Maity and T. S. Ray, *Prospects of Migdal Effect in the Explanation of XENON1T Electron Recoil Excess*, *Phys. Lett. B* **811** (2020) 135900 [2006.12529].
- [59] J. Smirnov and J. F. Beacom, *New Freezeout Mechanism for Strongly Interacting Dark Matter*, *Phys. Rev. Lett.* **125** (2020) 131301 [2002.04038].
- [60] G. Choi, T. T. Yanagida and N. Yokozaki, *Feebly interacting $U(1)_{B-L}$ gauge boson warm dark matter and XENON1T anomaly*, *Phys. Lett. B* **810** (2020) 135836 [2007.04278].
- [61] O. G. Miranda, D. K. Papoulias, M. Tórtola and J. W. F. Valle, *XENON1T signal from transition neutrino magnetic moments*, *Phys. Lett. B* **808** (2020) 135685 [2007.01765].
- [62] M. Lindner, Y. Mambrini, T. B. de Melo and F. S. Queiroz, *XENON1T anomaly: A light Z' from a Two Higgs Doublet Model*, *Phys. Lett. B* **811** (2020) 135972 [2006.14590].
- [63] D. Aristizabal Sierra, V. De Romeri, L. Flores and D. Papoulias, *Light vector mediators facing XENON1T data*, 2006.12457.
- [64] C. Boehm, D. G. Cerdeno, M. Fairbairn, P. A. Machado and A. C. Vincent, *Light new physics in XENON1T*, 2006.11250.
- [65] A. N. Khan, *Can Nonstandard Neutrino Interactions explain the XENON1T spectral excess?*, *Phys. Lett. B* **809** (2020) 135782 [2006.12887].
- [66] A. Bally, S. Jana and A. Trautner, *Neutrino self-interactions and XENON1T electron recoil excess*, *Phys. Rev. Lett.* **125** (2020) 161802 [2006.11919].
- [67] N. Sabti, J. Alvey, M. Escudero, M. Fairbairn and D. Blas, *Refined Bounds on MeV-scale Thermal Dark Sectors from BBN and the CMB*, *JCAP* **01** (2020) 004 [1910.01649].
- [68] A. Joglekar, N. Raj, P. Tanedo and H.-B. Yu, *Relativistic capture of dark matter by electrons in neutron stars*, 1911.13293.
- [69] K. Agashe, Y. Cui, L. Necib and J. Thaler, *(In)direct Detection of Boosted Dark Matter*, *JCAP* **10** (2014) 062 [1405.7370].
- [70] R. Harnik, J. Kopp and P. A. N. Machado, *Exploring ν Signals in Dark Matter Detectors*, *JCAP* **1207** (2012) 026 [1202.6073].
- [71] S. Bilmis, I. Turan, T. M. Aliev, M. Deniz, L. Singh and H. T. Wong, *Constraints on Dark Photon from Neutrino-Electron Scattering Experiments*, *Phys. Rev. D* **92** (2015) 033009 [1502.07763].
- [72] K. Kaneta, Z. Kang and H.-S. Lee, *Right-handed neutrino dark matter under the $B-L$ gauge interaction*, *JHEP* **02** (2017) 031 [1606.09317].
- [73] P. Ilten, Y. Soreq, M. Williams and W. Xue, *Serendipity in dark photon searches*, *JHEP* **06** (2018) 004 [1801.04847].
- [74] M. Bauer, P. Foldenauer and J. Jaeckel, *Hunting All the Hidden Photons*, *JHEP* **18** (2020) 094 [1803.05466].
- [75] M. Lindner, F. S. Queiroz, W. Rodejohann and X.-J. Xu, *Neutrino-electron scattering: general constraints on Z' and dark photon models*, *JHEP* **05** (2018) 098 [1803.00060].
- [76] N. Okada, S. Okada and Q. Shafi, *Light Z' and dark matter from $U(1)_X$ gauge symmetry*, *Phys. Lett. B* **810** (2020) 135845 [2003.02667].
- [77] G. Bellini et al., *Precision measurement of the ${}^7\text{Be}$ solar neutrino interaction rate in Borexino*, *Phys. Rev. Lett.* **107** (2011) 141302 [1104.1816].
- [78] TEXONO COLLABORATION collaboration, *Measurement of Neutrino-Electron Scattering Cross-Section with a CsI(Tl) Scintillating Crystal Array at the Kuo-Sheng Nuclear Power Reactor*, *Phys. Rev. D* **81** (2010) 072001 [0911.1597].
- [79] CHARM-II collaboration, *Measurement of differential cross-sections for muon-neutrino electron scattering*, *Phys. Lett.* **B302** (1993) 351.
- [80] CHARM-II collaboration, *Precision measurement of electroweak parameters from the scattering of muon-neutrinos on electrons*, *Phys. Lett.* **B335** (1994) 246.
- [81] J. Redondo and G. Raffelt, *Solar constraints on hidden photons re-visited*, *JCAP* **08** (2013) 034 [1305.2920].
- [82] J. B. Dent, F. Ferrer and L. M. Krauss, *Constraints on Light Hidden Sector Gauge Bosons from Supernova Cooling*, 1201.2683.
- [83] D. Kazanas, R. N. Mohapatra, S. Nussinov, V. L. Teplitz and Y. Zhang, *Supernova Bounds on the Dark Photon Using its Electromagnetic Decay*, *Nucl. Phys. B* **890** (2014) 17 [1410.0221].
- [84] J. D. Bjorken, S. Ecklund, W. R. Nelson, A. Abashian, C. Church, B. Lu et al., *Search for Neutral Metastable Penetrating Particles Produced in the SLAC Beam Dump*, *Phys. Rev. D* **38** (1988) 3375.
- [85] J. Blumlein et al., *Limits on neutral light scalar and pseudoscalar particles in a proton beam dump experiment*, *Z. Phys. C* **51** (1991) 341.
- [86] J. Blumlein et al., *Limits on the mass of light*

- (pseudo)scalar particles from Bethe-Heitler $e+e-$ and $\mu+\mu-$ pair production in a proton - iron beam dump experiment, *Int. J. Mod. Phys. A* **7** (1992) 3835.
- [87] M. Davier and H. Nguyen Ngoc, *An Unambiguous Search for a Light Higgs Boson*, *Phys. Lett. B* **229** (1989) 150.
- [88] E. M. Riordan et al., *A Search for Short Lived Axions in an Electron Beam Dump Experiment*, *Phys. Rev. Lett.* **59** (1987) 755.
- [89] T. Appelquist, B. A. Dobrescu and A. R. Hopper, *Nonexotic Neutral Gauge Bosons*, *Phys. Rev. D* **68** (2003) 035012 [[hep-ph/0212073](#)].
- [90] ALEPH, DELPHI, L3, OPAL, LEP ELECTROWEAK WORKING GROUP collaboration, *A Combination of preliminary electroweak measurements and constraints on the standard model*, [hep-ex/0612034](#).
- [91] M. Carena, A. Daleo, B. A. Dobrescu and T. M. P. Tait, *Z' gauge bosons at the Tevatron*, *Phys. Rev. D* **70** (2004) 093009 [[hep-ph/0408098](#)].
- [92] ATLAS collaboration, *Search for new high-mass phenomena in the dilepton final state using 36 fb^{-1} of proton-proton collision data at $\sqrt{s} = 13\text{ TeV}$ with the ATLAS detector*, *JHEP* **10** (2017) 182 [[1707.02424](#)].